DiVA
http://www.diva-portal.org

Postprint

This is the accepted version of a paper published in *ACS Applied Materials and Interfaces*. This paper has been peer-reviewed but does not include the final publisher proof-corrections or journal pagination.

Citation for the original published paper (version of record):

Wen, R-T., Niklasson, G A., Granqvist, C-G. (2015)
Strongly Improved Electrochemical Cycling Durability by Adding Iridium to Electrochromic Nickel Oxide Films.
ACS Applied Materials and Interfaces, 7(18): 9319-9322
https://doi.org/10.1021/acsami.5b01715

Access to the published version may require subscription.

N.B. When citing this work, cite the original published paper.

Permanent link to this version:
http://urn.kb.se/resolve?urn=urn:nbn:se:uu:diva-256240

Strongly improved electrochemical cycling durability by adding iridium to electrochromic nickel oxide films

Rui-Tao Wen, Gunnar A. Niklasson and Claes G. Granqvist*

Department of Engineering Sciences, The Ångström Laboratory, Uppsala University

P. O. Box 534, SE-75121 Uppsala, Sweden

KEYWORDS: electrochromic, Ir-Ni oxide, improved durability, charge density, optical modulation

ABSTRACT

Anodically coloring Ni oxide thin films are of much interest as counter electrodes in W-oxide-based electrochromic devices such as “smart windows” for energy efficient buildings. However, Ni oxide films are prone to suffer severe charge density degradation upon prolonged electrochemical cycling, which can lead to insufficient device lifetime. Therefore means to improve the durability of Ni-oxide-based films is an important challenge at present. Here we report that the incorporation of a modest amount of Ir into Ni oxide films [Ir/(Ir + Ni) = 7.6 at.%] leads to remarkable durability, exceeding 10,000 cycles in a Li-conducting

electrolyte, along with significantly improved optical modulation during extended cycling. Structure characterization showed that the *fcc*-type NiO structure remained after Ir addition. Moreover, the crystallinity of these films was enhanced upon electrochemical cycling.

Electrochromic thin-film devices are of much current interest for “smart windows” capable of varying their throughput of visible light and solar energy so that buildings can be rendered both energy efficient and comfortable.[1–3] These devices normally utilize joint transport of small ions and electrons between a thin film of tungsten oxide and a counter electrode based on nickel oxide, basically in the same way as in an electrical battery, and the optical transmittance is low when the charge resides in W oxide while the transmittance is high when the charge is in Ni oxide. Ni oxide films suffer from optical degradation and limitation in modulation span under extended electrochemical cycling,[4–6] and several recent studies aimed at alleviating these deficiencies have been reported. Beneficial effects of additives to the Ni oxide have been studied, specifically for Li,[7,8] C,[9,10] N,[11] W,[12] (Li,W),[13] (Li,Al),[14] (Li,Zr),[15] and several more. Nevertheless, the most crucial problem for Ni-oxide-based films, *viz*., their cycling durability, is still far from solved. In a previous paper,[4] we showed that the degradation of charge density in Ni-oxide follows a power-law decay model upon cycling in 1 M $LiClO_4$ dissolved in propylene carbonate (Li–PC), and long-term degradation hence does not only curtail cycle-life but also gradually erodes the optical modulation span of the device. In this Letter, we report that the charge density exchange in Ni-oxide-based thin films can be significantly *increased* during extended electrochemical cycling if the films contain a modest amount of iridium, and optical modulation is concomitantly enhanced.

We deposited Ir–Ni oxide films by co-sputtering from metallic iridium and nickel targets in argon–oxygen atmosphere onto unheated glass coated with In_2O_3:Sn (*i.e*., ITO, 60 Ω/square). Films were also prepared on carbon substrates for composition determination. Film thickness *t* was determined by surface profilometry across a step edge. The iridium content in the Ni oxide was characterized by Rutherford backscattering spectroscopy (RBS). Figure 1a shows RBS spectra of pristine Ni-oxide and Ir–Ni-oxide films and indicates that the iridium is homogeneously distributed over the film’s cross-section. Fitting the experimental data by use

of the SIMNRA program[16] yielded that Ir/(Ir + Ni) = 7.6 at.%. The film density was 5.6 g/cm^3. X-ray diffraction (XRD) patterns demonstrated that Ir–Ni oxide films have the same *fcc* structure as Ni-oxide (JCPDS No. 04–0385), as seen from Figure 1b. No diffraction peaks from IrO_2 or Ir were observed; rutile IrO_2 and metallic Ir would have yielded features at 28.1° and 34.7°, and at 40.1°, respectively. From the (200) diffraction peak, the grain size was estimated to be 13 nm and 21 nm for Ir–Ni oxide and Ni oxide, respectively. Expanded diffraction features in the 34–48° region revealed that peaks due to the (111) and (200) reflections shifted somewhat towards lower angles by Ir incorporation, thus indicating enlarged *d* spacing. Correspondingly, the cell volume for the Ir–Ni oxide is also slightly greater than that of Ni-oxide. This enlargement is in line with the expected structural variation when Ir atoms (radius 0.180 nm) replace Ni atoms (0.149 nm)[17] and may facilitate charge exchange as discussed later.

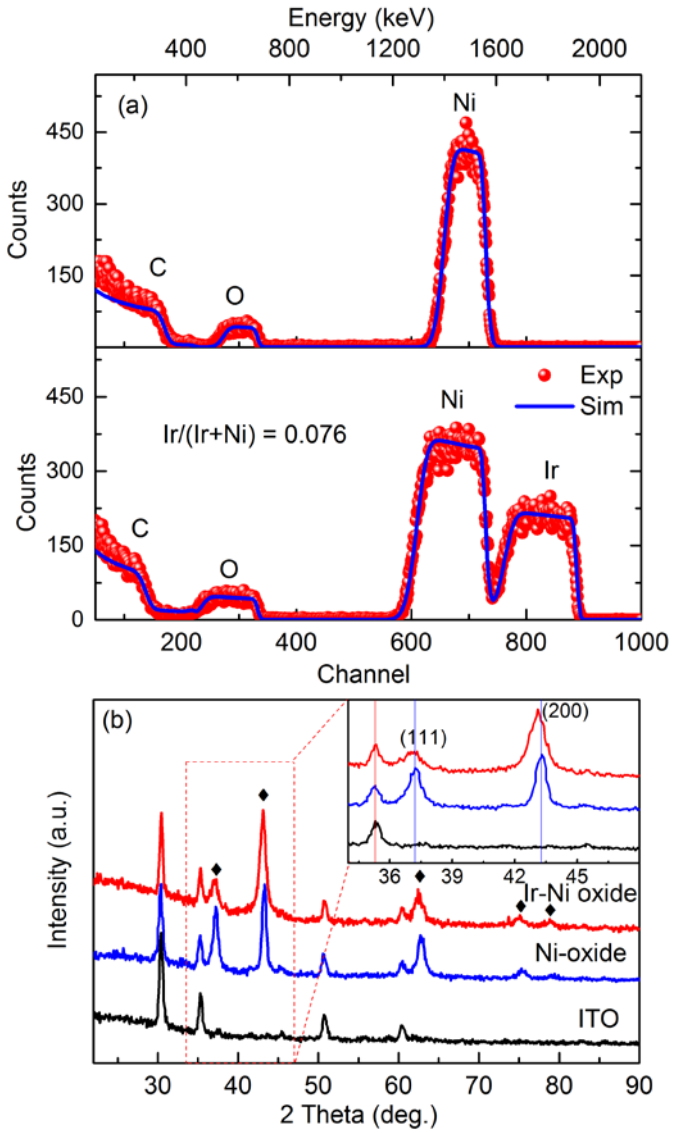

Figure 1. (a) Experimental and simulated RBS spectra for as-deposited thin films of Ni-oxide ($t \approx 180$ nm) and Ir–Ni oxide ($t \approx 270$ nm) on carbon substrates. The measurement used 2 MeV ^{4}He ions backscattered at an angle of 170°. Red dots are experimental results and blue lines are simulated spectra. (b) XRD characterization of Ni oxide and Ir–Ni oxide films; data for ITO are presented for comparison. Diffraction peaks agree well with the standard pattern of cubic NiO, as indicated by black diamonds. Inset is a close-up for the 34–48° region. Vertical blue lines serve as guidance for the eye. Vertical red line in the inset indicates that the peak due to ITO diffraction did not change. Data were taken by use of a Siemens D5000 instrument operating with CuK_α radiation at a wavelength of 0.0154 nm.

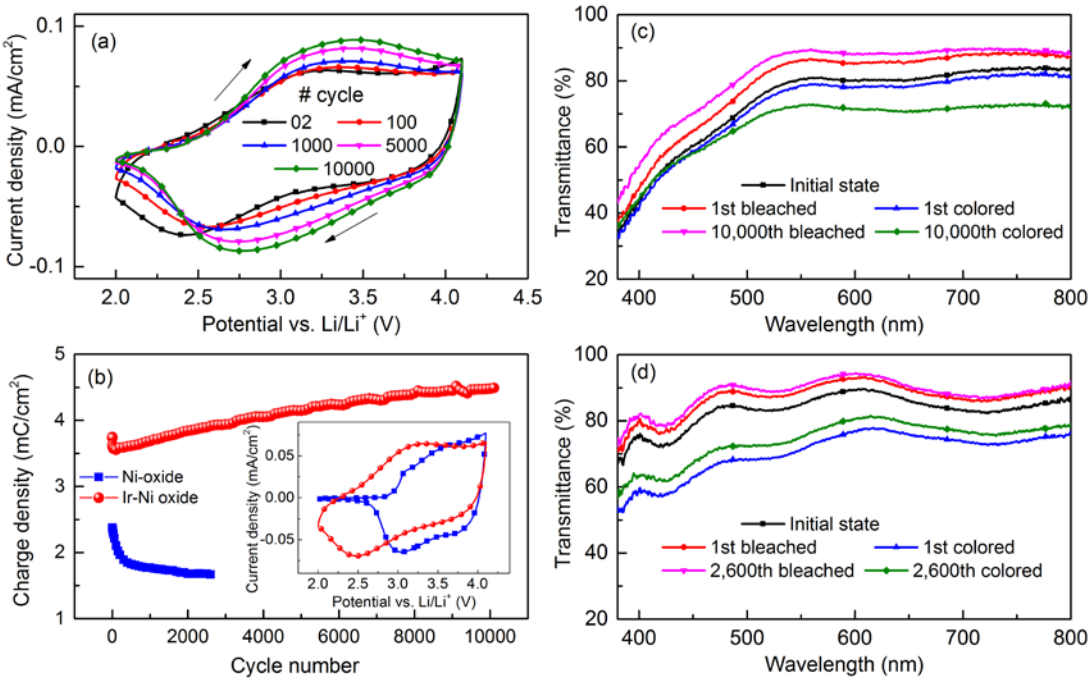

Figure 2. (a) Cyclic voltammograms for a thin film of Ir–Ni oxide ($t \approx 300$ nm) in 1 M Li–PC taken after the indicated number of cycles; the voltage sweep rate was 50 mV/s and arrows indicate sweep direction. (b) Charge density as a function of cycle number for the Ir–Ni oxide film and also for Ni oxide ($t \approx 250$ nm) in the voltage range 2.0–4.1V *vs* Li/Li^+ at 50 mV/s; inset shows CV curves for the corresponding films after five CV cycles. (c) and (d) Optical transmittance spectra for Ir–Ni oxide and Ni oxide before and after 10,000 and 2,600 CV cycles, respectively

We performed cyclic voltammetry (CV) measurements between 2.0 and 4.1 V *vs* Li/Li^+ in 1 M lithium perchlorate in propylene carbonate. *In situ* optical transmittance data in the wavelength (λ) range 380–800 nm were used to simultaneously record optical spectra before and after CV recordings. Figure 2a displays examples of cyclic voltammograms for an Ir–Ni oxide film for up to 10,000 cycles. It is evident that both anodic and cathodic peak currents increase substantially as cycling progresses. By integrating the inserted and extracted charge from the CV curves, it was found that the charge density grew monotonically for increased cycle number, apart from in the first few cycles (Figure 2b). This unexpected behavior points at extreme cycling durability for the Ir–Ni-oxide film. For the Ni oxide film, CV data taken

for 2,600 cycles were sufficient to reveal a strong loss of charge density (Figure 2b). The open circuit potential for Ir–Ni oxide was 3.13 V initially and increased to 3.25 V *vs*. Li/Li^+ after 10,000 cycles. In Ni oxide, this potential was 3.17 V initially and decreased to 3.09 V *vs*. Li/Li^+ after 2600 cycles.

The charge density for Ir–Ni oxide is obviously larger than for Ni oxide (Figure 2b), although the film thicknesses are similar. The larger cell volume, associated with the increased *d* spacing, is one reason that may facilitate the charge exchange. However, the main reason lies in different charge insertion and extraction processes. Specifically, most charge insertion and extraction take place between 2.7 and 4.1 V *vs* Li/Li^+ for pure Ni oxide (Figure 2b, inset), whereas insertion and extraction occur in the entire 2.0–4.1 V *vs* Li/Li^+ range for Ir–Ni oxide—as it does also for pure Ir oxide.[18] Thus we surmise that the increased charge density in the latter film is due to a contribution from Ir occurring primarily below 2.7 V. Enhanced charge density becomes even more pronounced for still larger Ir contents in the films (not shown). Optical transmittance spectra revealed that the optical modulation ($T_{\text{bleached}} - T_{\text{colored}}$) for Ir-Ni oxide is significantly enhancd from the initial 7.5% (at λ=550 nm) to 16.5 % at the $10{,}000^{\text{th}}$ cycle (Figure 2c), which is due to its increased charge density exchange upon cycling. It is also seen that the optical modulation of the Ir–Ni oxide film is somewhat smaller than that of a comparable Ni oxide film (Figure 2d), especially at short wavelengths where the introduction of Ir appears to introduce some extra absorption. Hence, the coloration efficiency for the Ir-Ni oxide film is also smaller than for the Ni oxide film, even after 10,000 cycles, because of the smaller optical modulation and larger charge density.

Scanning electron microscopy (SEM) was used to study possible morphological changes upon charge exchange between the Ir–Ni oxide film and the electrolyte. The SEM image exhibits a pristine film comprising small grains and cracks (Figure 3a). After 10,000 CV cycles, the morphology looks much the same (Figure 3b), which confirms that the surface structure is

stable. XRD data taken after 10,000 cycles showed that the film still exhibited the same *fcc* structure as in the initial state (Figure 3c). Using the (200) peak, the grain size was calculated from Scherrer's formula[19] to be ~13 nm for the film both before and after CV cycling. Detailed comparison of diffraction features revealed that peak intensities for the Ir–Ni oxide film became noticeably more distinct after electrochemical cycling, whereas the ITO-based features remained almost the same. We have at present no explanation for this unexpected result.

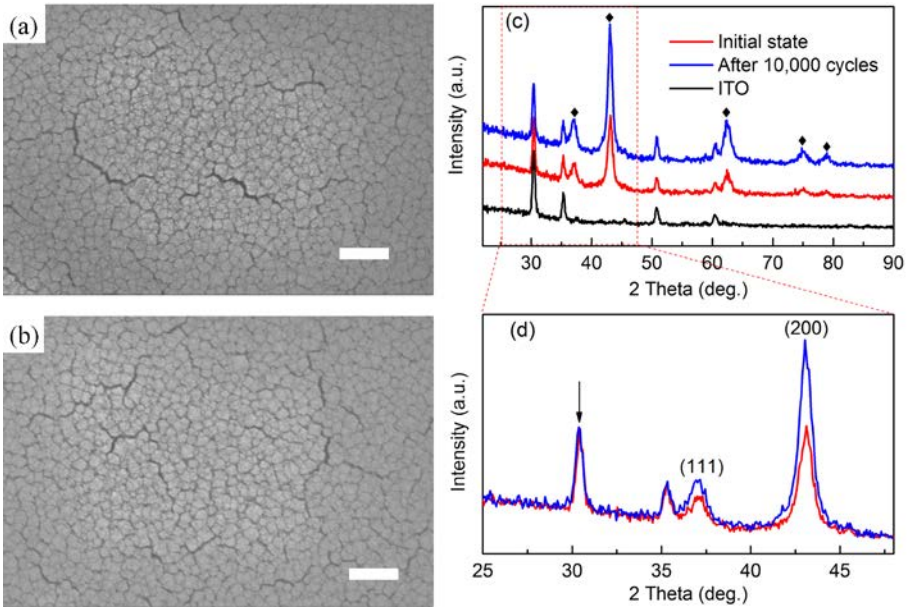

Figure 3. SEM images of an Ir–Ni oxide thin film (a) before and (b) after electrochemical cycling for 10,000 times between 2.0 and 4.1 V *vs* Li/Li^+. Data were recorded by use of a LEO 1550 FEG Gemini instrument with an acceleration voltage of 10 kV. The scale bars are 200 nm. (c) XRD pattern for an Ir–Ni oxide film before and after 10,000 CV cycles, and (d) close-up for the 25–48° range. Intensity curves (in arbitrary units, a. u.) are vertically displaced in (c). The blue arrow at ~30.4° in (d) indicates that the ITO peak has the same diffraction intensity before and after cycling.

Summarizing, we have demonstrated that charge density exchange, optical modulation and crystallinity improve in Ir–Ni oxide thin films subjected to extended electrochemical cycling in a Li^+-conducting electrolyte, whereas no similar effects are present in the absence of Ir. The

significance of these results is that Ir–Ni oxide thin films can yield a highly stable and reversible electochromic effect upon charge exchange and can serve as an excellent anode in W-oxide-based electrochromic devices. Further work is needed to ascertain the optimum Ir content for electrochromics-based applications.

AUTHOR INFORMATION

*Rui-Tao Wen

E-mail: Ruitao.Wen@angstrom.uu.se

Notes

The authors declare no competing financial interest.

ACKNOWLEDGEMENT: We acknowledge support with RBS-measurements from Daniel Primetzhofer and the staff of the Tandem accelerator laboratory at Uppsala University. Financial support was received from the European Research Council under the European Community's Seventh Framework Program (FP7/2007–2013)/ERC Grant Agreement No. 267234 ("GRINDOOR").

References

1 Granqvist, C. G. Handbook of Inorganic Electrochromic Materials; Elsevier, Amsterdam, The Netherlands, 1995.

2 Gillaspie, D. T.; Tenent, R. C.; Dillon; A. C. Metal-oxide Films for Electrochromic Applications: Present Technology and Future Directions. *J. Mater. Chem.* **2010**, *20*, 9585–9592.

3 Granqvist, C. G. Electrochromics for Smart Windows: Oxide-based Thin Films and Devices. *Thin Solid Films* **2014**, *564*, 1–38.

4 Wen, R.-T.; Granqvist, C. G.; Niklasson, G. A. Cyclic Voltammetry on Sputter-deposited Films of Electrochromic Ni oxide: Power-law Decay of the Charge Density Exchange. *Appl. Phys. Lett.* **2014**, *105*, 163502.

5 Wen, R.-T.; Niklasson, G. A.; Granqvist, C. G. Electrochromic Nickel Oxide Films and Their Compatibility with Potassium Hydroxide and Lithium Perchlorate in Propylene Carbonate: Optical, Electrochemical and Stress-related Properties. *Thin Solid Films* **2014**, *565*, 128–135.

6 Bouessay, I.; Rougier, A.; Poizot, P.; Moscovici, J.; Michalowicz, A.; Tarascon, J. M. Electrochromic Degradation in Nickel Oxide Thin Film: A Self-discharge and Dissolution Phenomenon. *Electrochim. Acta* **2005**, *50*, 3737–3745.

7 Kubo, T.; Nishikitani, Y.; Sawai, Y.; Iwanaga, H.; Sato, Y.; Shigesato, Y. Electrochromic Properties of Li_xNi_yO Films Deposited by RF Magnetron Sputtering. *J. Electrochem. Soc.* **2009**, *156*, H629–H633.

8 Tenent, R. C.; Gillaspie, D. T.; Miedaner, A.; Parilla, P. A.; Curtis, C. J.; Dillon, A. Fast-switching Electrochromic Li^+-doped NiO Films by Ultrasonic Spray Deposition. *J. Electrochem. Soc.* **2010**, *157*, H318–H322.

9 Lin, Y.-S.; Lin, D.-J.; Sung, P.-J.; Tien, S.-W. Atmospheric-pressure Plasma-enhanced Chemical Vapour Deposition of Electrochromic Organonickel Oxide Thin Films with an Atmospheric Pressure Plasma Jet. *Thin Solid Films* **2013**, *532*, 36–43.

10 Lin, Y.-S.; Lin, D.-J.; Chiu, L.-Y.; Lin, S.-W. Lithium Electrochromism of Atmospheric Pressure Plasma Jet-synthesized NiO_xC_y Thin Films. *J. Solid State Electrochem.* **2013**, *16*, 2581–2590.

11 Lin, F.; Gillaspie, D. T.; Dillon, A. C.; Richards, R. M.; Engtrakul, C. Nitrogen-doped Nickel Oxide Thin Films for Enhanced Electrochromic Applications. *Thin Solid Films* **2013**, *527*, 26–30.

12 Green, S. V.; Granqvist, C. G.; Niklasson, G. A. Structure and Optical Properties of Electrochromic Tungsten-containing Nickel Oxide. *Sol. Energy Mater. Sol. Cells* **2014**, *126*, 248–259.

13 Gillaspie, D.; Norman, A.; Tracy, C. E.; Pitts, J. R.; Lee, S.-H.; Dillon, A. Nanocomposite Counter Electrode Materials for Electrochromic Windows. *J. Electrochem. Soc.* **2010**, *157*, H328–H331.

14 Lin, F.; Nordlund, D.; Weng, T. C.; Moore, R. G.; Gillaspie, D. T.; Dillon, A.; Richards, R. M.; Engtrakul, C. Hole Doping in Al-containing Nickel Oxide Materials to Improve Electrochromic Performance. *ACS Appl. Mater. Interfaces* **2013**, *5*, 301–309.

15 Lin, F.; Nordlund, D.; Weng, T. C.; Sokaras, D.; Jones, K. M.; Reed, R. B.; Gillaspie, D. T.; Weir, D. G. J.; Moore, R. G.; Dillon, A.; Richards, R. M.; Engtrakul, C. Origin of Electrochromism in High-performing Nanocomposite Nickel Oxide. *ACS Appl. Mater. Interfaces* **2013**, *5*, 3643–3649.

16 Mayer, M. SIMNRA, A Simulation Program for the Analysis of NRA, RBS and ERDA. *Am. Inst. Phys. Conf. Proc.* **1999**, *475*, 541–544.

17 Clementi, E.; Raimondi, D. L. Atomic Screening Constants from SCF Functions. *J. Chem. Phys.* **1963**, *38*, 2686–2689.

18 Wen, R.-T.; Niklasson, G. A.; Granqvist, C. G. Electrochromic Iridium Oxide Films: Compatibility with Propionic Acid, Potassium Hydroxide, and Lithium Perchlorate in Propylene Carbonate. *Sol. Energy Mater. Sol. Cells* **2014**, *120*, 151–156.

19 Cullity, B. D.; Stock, S. R. Elements of X-ray Diffraction, third ed., Prentice-Hall: Upper Saddle River, NJ, 2001.

Table of Contents